Large-scale high-resolution simulations of high gain direct-drive inertial confinement fusion targets

Andrew J. Schmitt,* D.G. Colombant, A.L. Velikovich, and S.T. Zalesak
Plasma Physics Division, Naval Resarch Laboratory, Washington DC 20375-5346

J.H. Gardner and D.E. Fyfe
LCP&FD, Naval Research Laboratory, Washington DC 20375-5344

N. Metzler
SAIC, McLean VA

Targets have been designed that produce moderate to high gain when directly driven by lasers. The intrinsic sensitivity of these targets to hydro instabilities is found using the FAST(2D) multidimensional radiation hydrocode [J.H. Gardner, A.J. Schmitt, J.P. Dahlburg, *et al.*, Phys. Plasmas **5**, 1935 (1998)], which simulates the simultaneous behavior of a large bandwidth (e.g., $\ell = 2 - 256$) of perturbations from compression to acceleration, and then to stagnation and burn. The development of the structure in these multi-mode simulations is benchmarked to theoretical analysis and single-mode calculations, which reveals the need to "renormalize" the simulation after compression. The simulations predict that a direct drive point design is expected to degrade significantly from its 1-D clean yield, yet still ignite and give appreciable gain. Simulations of high-gain pellets using a spike prepulse to inhibit Richtmyer-Meshkov growth show a considerable robustness, with high (> 100) gains possible even with nominal surface finishes and laser imprint.

I. INTRODUCTION

Laser-driven inertial confinement fusion (ICF) is difficult to achieve because the implosion process is inherently hydrodynamically unstable: a hot low-density plasma is used to compress and accelerate a cold high-density plasma. Thus control of these hydrodynamic instabilities are essential to the success of ICF. Current experimental facilities are insufficient to directly test the effects of these instabilities on ignition and gain, so simulations are extremely important.

We present here the status of our ICF implosion simulations using our FAST code[1]. Of general interest is to quantify the allowable perturbations (from surface finish or optically-smoothed laser drive) which can be tolerated. We wish to be able to simulate the degradation of yield as pellet nonuniformities are varied, and in particular determine whether the yield of ICF pellets will remain high when we apply nominally known imperfections in surface finishes and laser imprint.

A necessary condition for this result is to determine, from simulations or other analysis, the growth rates and behavior of very low amplitude single-mode perturbations. The analysis or simulation must include growth from such disparate effects as the Richtmyer-Meshkov (RM) instability[2], feed-out of perturbations from one side of the target to the other[3], Rayleigh-Taylor (RT) instability[4], and Bell-Plesset effects[5]. All of these must be considered during the initial compression of the target, its acceleration, and then its deceleration when it stagnates in the core region. For mild nonlinear amplitudes, estimates like the Haan-saturation approximation may be performed. The resulting growth factors can be applied to known initial spectra of perturbations and, as long as the amplitude of each mode remains fundamentally linear, the final net amplitude can be determined as the linear sum of the individual modes after growth. To estimate the effect these final perturbations have on gain, either analytic[6] or simulation[7] approximations must be provided. Unfortunately, the final perturbations are typically not at the linear amplitude level assumed in the models. We chose instead to attempt to model the entire implosion from beginning to end.

Simulation of the full implosion from beginning to end is computationally difficult, particularly for direct-drive ICF. Compared to indirect-drive ICF[8], direct drive has unique perturbation sources (e.g., imprint from the optical smoothing of the laser drive) and less ablative stabilization of the Rayleigh-Taylor growth rate. For both reasons, the growth factors for perturbations in directly-driven implosions peak at relatively short perturbation wavelength (Legendre mode numbers in the region of 100-200, corresponding to perturbation wavelengths of order 100 μm). Thus one challenge is that high resolution simulations must be performed. In the two-dimensional (2D) simulations shown here, 300-500 points are used in the radial direction, and 2048 in the angular direction. For a full pellet, the representable modes are thus $\ell = 1 - 1024$, but because of unavoidable numerical diffusion we consider only the range $\ell = 1 - 256$ to be adequately resolved. Another challenge is the low levels of initial perturbations compared to the final level. For instance, optically smoothed light using many overlapped beams and large (~ 1 THz) bandwidth produces perturbations on the pellet that are equivalent to a few Angstroms of amplitude per mode. This scale size is much smaller than even the final imploded pellet scales. The code uses sliding-zone Eulerian gridding to keep small grid spacing in the regions of small perturbations; however, even this technique cannot fully resolve all of this structure. For the presentations here, we resort instead to a renormalization technique described in the next section. We are also developing numerical algorithms which are able to accurately simulate the extremely small perturbations involved

*Electronic address: andrew.schmitt@nrl.navy.mil

in this problem.

II. THE SIMULATION PROCESS

For the purposes of analysis, the laser ICF problem is separated here into the compression and acceleration phases. Separate analysis of the subsequent stagnation and burn phases will be left to a future paper. Although the pellet is hydrodynamically unstable during both compression and acceleration, the quantitative and qualitative details of these phases are different. The compression phase is characterized by the mildly growing and oscillating Richtmyer-Meshkov instability, while the acceleration phase is dominated by the exponentially growing Rayleigh-Taylor instability.

A. Compression phase: Richtmyer-Meshkov

In the compression phase, a shock is launched on the outside of the ablator by a relatively low-intensity portion of the laser pulse. The purpose of this shock is to compress the ablator and fuel in the pellet and heat it to the point that it can withstand the drive portion of the pulse without appreciable increase in its adiabat. This phase ends when this shock breaks out of the rear of the pellet shell. Any perturbations or contact-discontinuities it encounters before then are susceptible to the Richtmyer-Meshkov (RM) instability. In addition, the optically-smoothed laser introduces a constant source of pressure fluctuations to the compressing shock. The resulting ablatively-driven RM instability is characterized by first growing and then oscillating and damped perturbations.

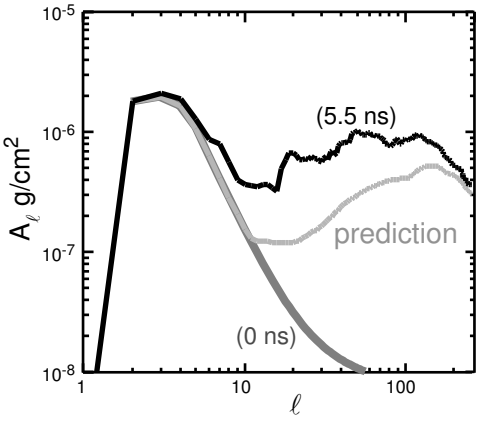

FIG. 1: Areal mass perturbation spectrum in the simulation as a function of Legendre ℓ mode is shown at t=0 (dark gray) and near the end of the compression phase (black). The light gray curve shows the predicted maximum value based upon analytic benchmarks and larger amplitude single-mode simulation.

We have used the recently developed ablatively-stabilized RM theory[2] to benchmark single-mode simulations of simple (all-Deuterium-Tritium (DT)) pellets[9]. These simulations follow either surface perturbations or imprint from optically smoothed lasers (e.g., induced-spatial-incoherence (ISI)[10] or smoothing by spectral dispersion (SSD)[11] methods). The amplitude of the perturbation is made large enough to resolve (e.g., 1000Å) but small enough to stay in the linear regime. (The linear theory expansion parameter, ka_0, where k is the perturbation wavelength and a_0 is the perturbation amplitude, is of order 0.1 to 1.0% in these single-mode studies.) For the benchmarks of optical smoothing, five simulations at each perturbation wavelength were performed using well defined single-beam laser perturbations[12]) and averaged in order to reduce statistical fluctuations in the results. These single-mode benchmarks have been compared to the linear ablatively-stabilized RM theory and have been shown to produce very similar growth factors and oscillation behavior[9], and also exhibit linear behavior when the initial amplitudes are varied. These single-mode simulations were cross checked with small multimode simulations containing eight resolved modes of the same approximate amplitude (~ 500Å), and the time behavior of each individual mode was verified to be very close to that of the single-mode simulation of the corresponding wavelength. However, when the mode amplitudes become much smaller than the grid spacing, and the number of resolved modes is much larger, the fidelity of the simulations deteriorates (as we see in the next section).

The single-mode simulation results are used to construct a prediction for the areal-mass perturbations expected at the end of the compression phase. The maximum areal-mass perturbation level during compression is recorded, and interpreted as either a growth factor (for surface perturbations) or equivalent surface perturbation (for the laser imprint). The maximum value (as opposed to, say, the instantaneous value at the end of compression) is used to give a conservative (as opposed to optimistic) prediction. The resulting growth-factor or imprint-efficiency is used to predict the areal-mass perturbations at the end of the compression phase given a surface perturbation spectrum and optically-smoothed laser spectrum (determined by its bandwidth, focal spot size, laser f-number, etc.[12]).

The next step is to compare a high-resolution multi-mode simulation of the pellet during the compression phase to the maximum levels predicted by the growth-factors and imprint efficiency results of the single-mode runs. An example is a simulation of the all-DT NIF pellet point design [9, 13] where the outer surface is initialized with the National Ignition Facility (NIF)-standard specification spectrum[14] and the driving 0.35 μm laser is optically smoothed with 1 THz bandwidth. In these simulations, modes 1-256 are considered well resolved (there are 2048 points in the theta direction, and 16 points are believed to be needed to resolve a mode properly without numerical diffusion). The difference between this and the earlier benchmarks is both the larger range of modes considered, and the much smaller amplitude of individual modes (as small as 1Å). Fig. 1 shows the spectrum of areal mass perturbations at t=0 and at the time of shock breakout at 5.5 nsec in the simulation. We can compare this to the expected level, found as the rms sum of the initial surface amplitude (multiplied by the growth factor) and the equivalent laser imprint. This shows that these highly resolved multimode calculations

significantly overestimate the areal mass perturbations at the end of compression. This is overestimation, not new physics, because these results are inconsistent with both linear RM theory and the carefully benchmarked single-mode simulations.

There are a variety of reasons for this. First, the perturbation levels per mode (as small as 1-10 Å) are much smaller than both the larger amplitude single-mode simulations and the typical grid size (1000Å) used to resolve the perturbations. Secondly, the initial conditions involve a 2D density discontinuity that is not aligned to the orthogonal mesh; this necessarily contains higher harmonics of the modes that are being represented[15]. These harmonics can generate nonphysical perturbations (through the nonlinear hydrodynamic algorithms) that interfere with and artificially inflate the initially driven (and extremely small) fluctuations at those harmonics. We are currently modifying the algorithms in the code to accurately calculate these extremely small signals (see section IV), but those methods are not yet available to the multimode simulation code.

The approach taken here to bypass the problem of artificially high perturbation levels at the end of compression is to filter the offending fluctuation levels. This filtering is done (once at the end of compression) on all the fundamental simulation variables with a filter that is a function of the Legendre ℓ mode only. At every radial point that has been overtaken by the first shock (this does not include the inner surface perturbations), the plasma variables (density, velocities, and energy density) are decomposed into their spectral components in Legendre space, multiplied by the filter function, and then reconstructed. This filter function is constructed from the ratio of the expected areal mass perturbation amplitude to the simulation areal mass amplitude at each Legendre mode: $f(\ell) = d\rho R(\ell)_{expected}/d\rho R(\ell)_{simulation}$. This ensures that the important acceleration phase begins with roughly the expected amplitudes between the perturbations in mass density, velocity, and energy density. However, since some portion of the perturbation may be noise-driven, the radial structure of the perturbation may be different than it should be. Samples of the radial structure of the individual modes does not reveal obvious qualitative differences with the single-mode results. Also, other tests have not shown differences in Rayleigh-Taylor growth rates during the subsequent acceleration phase. We believe that this procedure provides a reasonable starting point for the next phase of the implosion, the exponentially unstable acceleration phase.

B. Acceleration phase: Rayleigh-Taylor

The acceleration phase starts when the rarefaction wave from the rear surface of the pellet reaches the front surface of the pellet, and the front surface begins to accelerate. During this phase, perturbations on the outer edge of the pellet are expected to grow exponentially. Rayleigh-Taylor (RT) theory[16] states that any perturbation is composed of both growing and decaying eigenmodes; the amplitude of the growing eigenmodes (localized to the region near the ablation surface) quickly eclipse the decaying modes and dominate the resulting instability behavior. Unlike the classical RT instability, laser-driven RT is ablatively stabilized if the perturbation wavenumber of the perturbation is large (typically $\ell \gtrsim 100$). This is a simplification of the actual case where dynamic effects such as the intensity (drive pressure) increase and equilibration waves/shocks also influence the behavior, but the essential physics is the same.

Benchmarks have been done to compare the growth of perturbations in the multimode simulations to that expected by the dispersion relations given by common ablatively stabilized RT models[16–18]. For instance, when the previous all-DT NIF pellet simulation is allowed to progress into the acceleration phase, we can compare mode-by-mode the development of the areal mass perturbation with the RT dispersion relations (Fig.2). In the example shown here, we use the modified Bodner-Takabe (MBT) dispersion relation[4, 18] $\gamma(t) = \sqrt{kg/(1-kL_D)} - k\beta V_{abl}$ (with $\beta = 3$) and integrate it in time using the (time dependent) ablation velocity, acceleration, and ablation density scale-length given by the equivalent one-dimensional simulation of the pellet implosion. Nonlinear growth ($a_0/\lambda > 0.1$) is approximated as secular growth according to the Haan prescription[19]; convergence effects are handled by a simplified incompressible Bell-Plesset model which includes amplitude growth $\sim R^{-2}$. The growth of the modes in the simulation is quite similar to that expected, at least until nonlinearity becomes important (about 8.5 nsec). These comparisons indicate that the FAST code is accurately simulating the rapid growth of the Rayleigh-Taylor instability during acceleration. This increases our confidence in the ability of the code to correctly predict the assembly of the core undergoing ignition and burn.

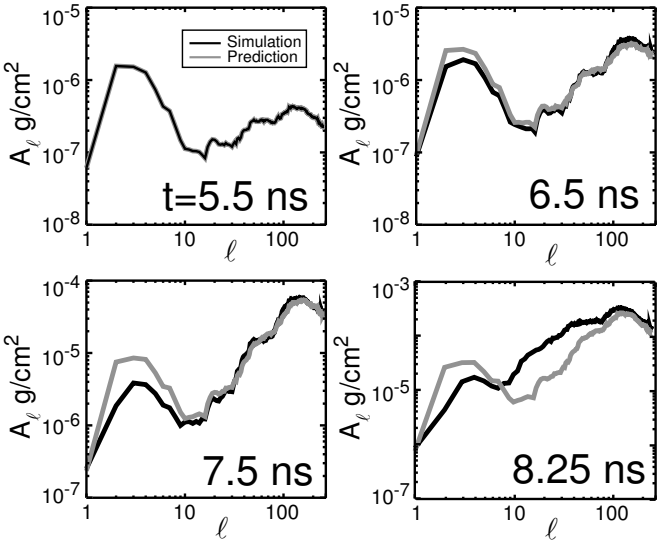

FIG. 2: Areal mass perturbation spectrum in the simulation as a function of Legendre ℓ mode is shown at different times through the acceleration phase of the simulation. The gray lines show the predictions from the RT dispersion relation (starting with the simulation perturbation spectrum at the end of the compression phase), while the black lines denote the simulation results.

III. SIMULATION RESULTS

A. All-DT NIF point design

We began the comparisons by showing the all-DT NIF pellet and the development of its individual modes during the compression and acceleration phase. It is instructive then to examine the results of this simulation when it runs fully through ignition and burn. Fig.3 a shows the results of this pellet when only outer surface perturbations and 1THz of optically smoothed light are considered; the images of the mass density for two different times near ignition show a fairly round shell with perturbation structures that are mostly confined to the outer 50% of the pellet. In this case, the code predicts a gain of about 24, which is about 70% of the "clean 1D" prediction. If we add a nominal 1 μm RMS of inner surface nonuniformity, the gain drops to 17, or about 50% of clean 1D (Fig.3 b). Further adding a constant-in-time low-mode asymmetry to account for beam misalignment and power imbalance[20], the simulation shows a significant residual P_2 asymmetry (Fig.3 c) which results in appreciably smaller gain (5).

B. High-Gain KrF driven designs

We have also designed a target to be driven by a 2.5 MJ KrF laser to high gain (defined as greater than 100, in this case ~ 150). This target takes advantage of the high coupling efficiency provided by the very absorptive 0.25 μm laser light and the ability to zoom (shrink the laser spot size) at two different times during the implosion. (The laser spot is shrunk to match the critical surface diameter at the zoom times). The zooming contributes to the high coupling efficiency since it minimizes refractive losses of the laser light during the main drive portion of the pulse and keeps the absorbed laser energy close to the ablation surface. Also, because the pellet surface is shrinking along with the laser spot size, the total laser power can be decreased at the same time without a concomitant decrease in drive pressure. The design specifications are shown in Fig.4. The pellet is driven with a shaped laser pulse that optionally has a spike prepulse at the very start. This spike prepulse is configured to decrease the pellet's sensitivity to laser imprint and outer surface nonuniformity[21] without significantly affecting the fuel adiabat in the imploding pellet. Differently configured spikes can also be used to preferentially heat the pellet ablator and increase the ablative stabilization of the Rayleigh-Taylor instability by increasing the ablation velocity[22, 23]. Analysis of 1D simulations of this pellet show that the RT instability for this pellet with the two different laser pulses is quite similar (Fig.5), although the spike does produce minor stabilization increases at the largest ℓ. The average adiabat as a function of time also shows relatively little difference. Thus, we expect that the major effect of the spike in the pulse is to decrease the RM growth of surface perturbations and leave a smaller seed perturbation for the later RT growth to amplify.

The two dimensional stability and gain of this pellet is

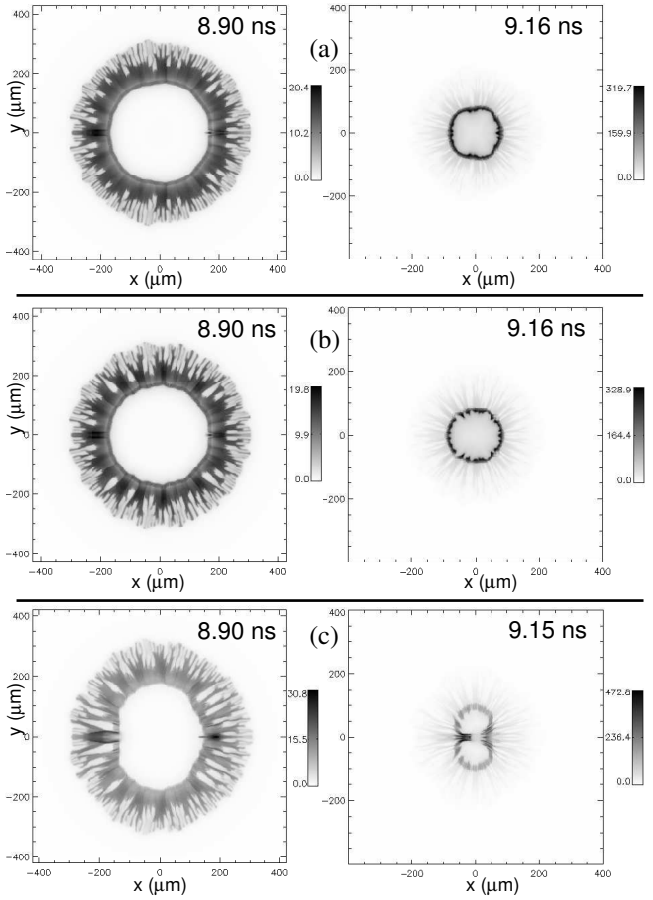

FIG. 3: Three series of simulation density images at roughly the same late times showing the effects of increasing perturbation contributions on the all-DT NIF point design pellet. (a) Outer surface perturbation ($\sigma_{RMS} = 0.125\mu m$) and 1 THz optically-smoothed light; (b) adding $1.0\mu m$ RMS Inner surface perturbation; (c) additionally adding 2% low-mode asymmetry to the laser drive. The gain drops from the 1D value of 35 to (a) 24; (b) 17; (c) 5.

simulated by the compression/ renormalization/ acceleration method presented earlier. Again, the growth factor and imprint efficiencies are calculated during compression for the two different laser pulses with well-resolved single-mode simulations. As shown in Fig.6, these show that the spike prepulse decreases the surface perturbation growth by a factor of ten for some wavenumbers. In contrast, the net laser imprint after compression is not reduced by the spike, probably because of the short-averaging time of the optically-smoothed spike, but the perturbations at the end of compression are dominated by surface perturbations. Combining this with the similar RT growth factors, we expect the spike stabilized pellet to perform better.

Indeed, the improvement in the compression phase stabilization significantly affects the projected performance of the pellet. We again apply the NIF-standard outer surface finish spectrum to the pellet and drive it with a KrF laser smoothed by 1 THz of ISI. The resulting simulations show that without the spike prepulse, the perturbations produced by the end of compression grow large enough to prevent the pellet from sig-

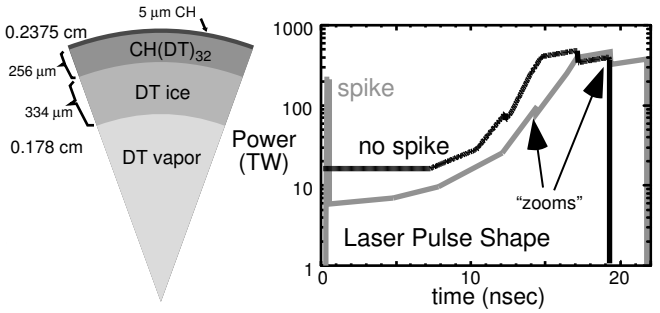

FIG. 4: Design specifications for (a) the KrF-driven high-gain pellet, and (b) constant-foot (black) and spike prepulse (gray) laser drive. At the points marked "zoom" in (b), both the laser spot size and its total power is decreased. The spot size at these times (in both cases) is shrunk by the ratios 0.8 and 0.54 compared to the initial spot size (which is equal to the initial pellet diameter, 0.475 cm).

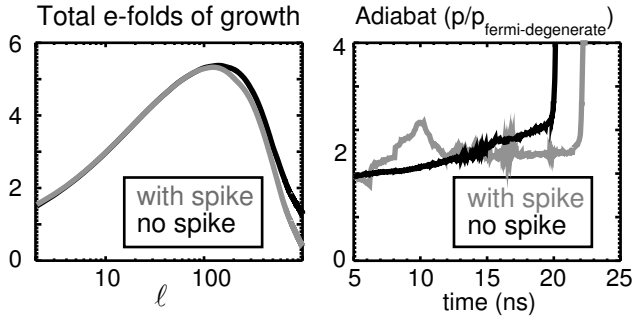

FIG. 5: Projected growth factors during for the acceleration phase (RT) of the high gain pellet, for the constant-foot (black) and spike prepulse (gray). Also shown are the adiabat of the pellet, averaged over the region between 1/e and 1 times the maximum fuel density.

nificantly igniting, and the gain is less than unity (Fig.7(a)). In contrast, with a spike prepulse and despite the addition of $1\mu m$ rms perturbations on the DT-ice inner surface layer, the perturbations are confined to a relatively small area on the outside of the pellet throughout the implosion (with the noticeable exception of a small bubble on the pellet's axis that penetrates through to the interior)(Fig.7(b)). The final yield in this latter case decreases less than 10% from its clean 1D value (160).

Although the spike prepulse clearly reduces the RT seeds, the differences in the instability growth in the pellets with and without the spike are larger than expected due to just the lower seeding. If we look at a time in both pellets that is close to the maximum acceleration, and compare the perturbation spectrum to that which we would expect (given the simple MBT-RT dispersion relation noted earlier), we find an apparent discrepancy (Fig.8). In particular, the growth in the pellet with no spike is significantly greater than the level expected (up to an order of magnitude greater). It is unknown at this time whether this is simply due to the simplifications involved in the RT formula, or is a reflection of the limits of either the current analysis or this more complex layered target (compared to all-DT). For instance, we can sometimes expect a smaller than expected perturbation due to the finite time it can take

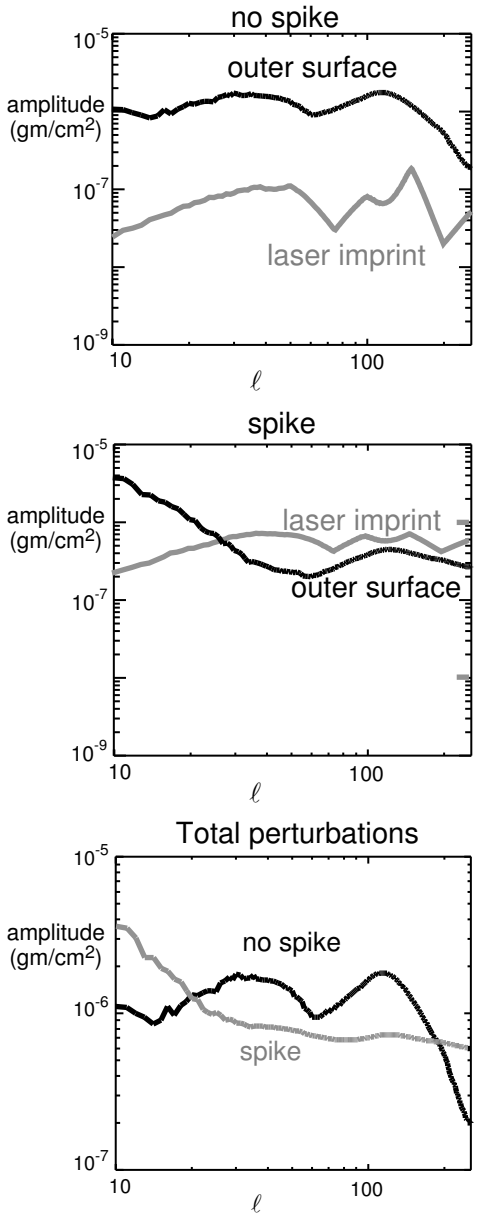

FIG. 6: Projected amplitude after the compression phase (RM) of the high gain pellet, assuming a NIF standard initial surface spectra and 1THz of optically smoothed light. Shown are the contributions from the surface perturbations and laser imprint for (a) the constant-foot pulse (no spike); and (b) the pulse with spike. The total perturbations at the end of compression for both cases are compared in (c).

for an RT eigenmode to become established[9]. The study of these simulations are ongoing.

IV. FUTURE IMPROVEMENTS

One of the largest uncertainties in this study is the effect of the renormalization on the results presented here. It would be greatly desirable to rid ourselves of this approximation entirely. This section summarizes our work in this area, with

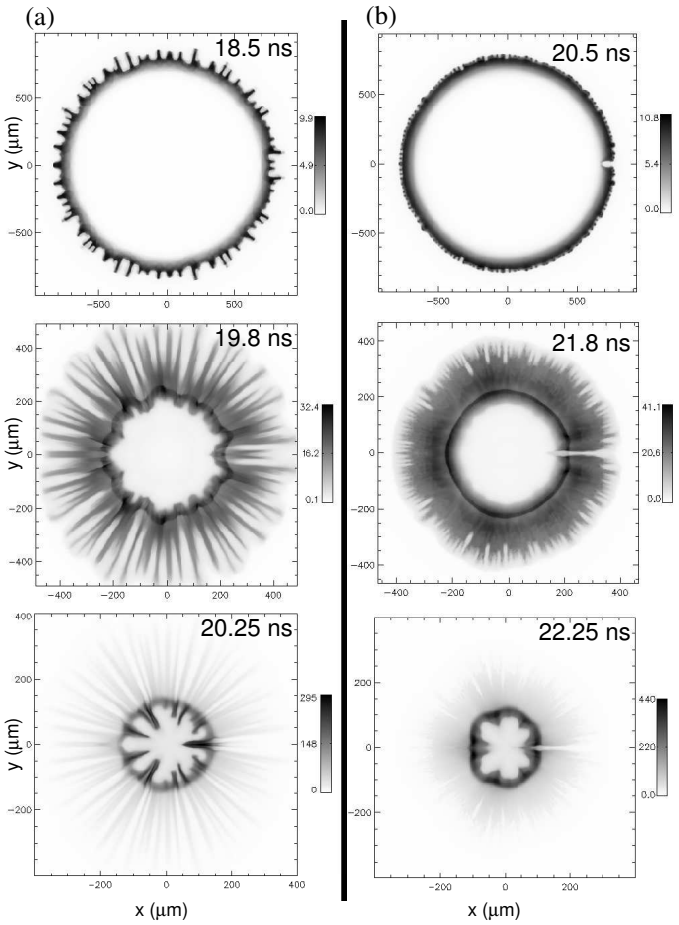

FIG. 7: Simulation results showing density images at three times towards the end of the implosion for the (a) no spike prepulse and (b) spike prepulse designs.

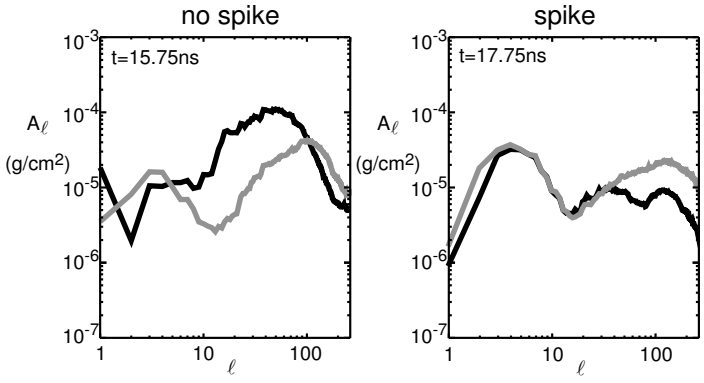

FIG. 8: The spectrum of perturbations from the simulation in both (a) no spike prepulse and (b) spike prepulse designs is compared to the values predicted using the MBT RT dispersion formula and the actual seeds at the start of the acceleration phase. The gray lines show the predictions from the RT dispersion relation (starting with the simulation perturbation spectrum at the end of the compression phase), while the black lines denote the simulation results.

details to be presented in another publication[24].

It was previously noted that one of the sources of numerical noise for very low amplitude perturbations was the early development of mode-coupling and hence nonlinearity. Unfortunately, nonlinearity, and more important non-differentiability is inherent in modern higher-order (2nd or more) monotone shock-capturing algorithms such as the flux-corrected-transport (FCT) algorithms used in the FAST code. We are developing numerical methods that preserve the differentiability and linearity of small perturbations in the simulation codes, and allow accurate multimode simulation of tiny perturbations. By necessity, any physical linear algorithm must be first order in time and space[25]. The method must also clearly be able to handle shocks as well, however. Thus the desirable algorithm must be linear and differentiable in the regions of flow outside of discontinuities (like shocks), yet be able to be nonlinear where the flow is nonlinear. As an example, the results of a first-order Godunov method (in radius) combined with a two-step Lax-Wendroff algorithm (in the direction orthogonal to the shock propagation) are presented in Fig.9. This is from an ablative-RM simulation of a single $24\mu m$ wavelength perturbation on the edge of a DT-ice shell. It has an initial amplitude of $5 \times 10^{-9} cm$ and is driven by a constant intensity pulse. Also shown in the figure is the "noise" in the perturbation, defined as the rms sum of all perturbation fluctuations at wavelengths different from the seeded mode. The signal-to-noise ratio remains greater than 4 orders of magnitude throughout the simulation. The simulation shown assumes an ideal equation of state and a single fluid temperature. Algorithms similar to this, additionally capable of handling multiple materials, two fluid temperatures, and general equations of state, are being integrated into the FAST code, where we will use them to simulate the compression phase of the pellet.

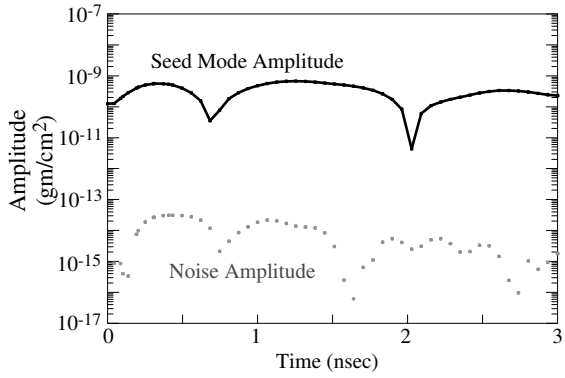

FIG. 9: The evolution of a single-mode $24\mu m$ wavelength with initial amplitude $5 \times 10^{-9} cm$ as computed by a first-order Godunov scheme in the radial direction (along the direction of propagation) combined with a Lax-Wendroff scheme in the orthogonal direction. Also shown is the evolution of the noise, which is defined as the rms sum of all perturbations in the simulation that are not at the fundamental wavelength ($24\mu m$).

V. CONCLUSIONS

We have analyzed the implosion of direct drive pellets with highly resolved multimode simulations. Careful benchmarking of the code is needed to bypass problems involving numerical noise. We analyze the compression and acceleration phases of the implosion separately, and compare to analytic theory and well resolved benchmarks. These comparisons reveal the need to renormalize the simulation at the end of the compression phase. The resulting simulations show appreciable degradation of uniformity and gain in the all-DT NIF pellet design and a high-gain KrF laser driven design. However, the addition of a spiked prepulse in the high-gain design significantly reduces the final irregularities and distortions of the imploded pellet. With nominal (NIF-spec.) inner and outer surface finishes and imprint from optically smoothed light, the stabilized high-gain pellet produces nearly full clean 1D pellet gain of over 150. Low-mode asymmetries due to beam imbalance or mispointing and 3-D simulations are still yet to be done; however, these results indicate that energy production from ICF targets directly driven by short-wavelength lasers may be a viable possibility in the future.

Acknowledgments

We thank Keith and Steve Obenschain for their support in providing the advanced computer clusters needed for this work. This work was supported by U.S. Department of Energy.

[1] J.H. Gardner, A.J. Schmitt, J.P. Dahlburg *et al.*, Phys. Plasmas **5**, 1935 (1998).
[2] V.N. Goncharov, Phys. Rev. Lett. **82**, 2091 (1999); A.L. Velikovich, J.P. Dahlburg, J.H. Gardner, and R.J. Taylor, Phys. Plasmas **5**, 1491 (1998); R. Ishizaki and K. Nishihara, Phys. Rev. E **58**, 3744 (1998).
[3] A.L. Velikovich, A.J. Schmitt, J.H. Gardner, and N. Metzler, Phys. Plasmas **8**, 592 (2001); R. Betti, V. Lobatchev, and R.L. McCrory, Phys. Rev. Lett. **81**, 5560 (1998).
[4] J. D. Lindl, Inertial Confinement Fusion (Springer-Verlag, New York, 1998).
[5] G. I. Bell, "Taylor instability on cylinders and spheres in small amplitude approximation," Los Alamos Scientific Laboratory Report No. LA-1321, 1951; M. S. Plesset, J. Appl. Phys. **25**, 96 (1954).
[6] R. Kishony and D. Shvarts, Phys. Plasmas **8** 4925 (2001).
[7] P. McKenty, V.N. Goncharov, R.P.J. Town, S. Skupsky, R. Betti, and R.L. McCrory, Phys. Plasmas **8** 2315 (2001).
[8] M.M. Marinak, R.E. Tipton, O.L. Landen *et al.*, Phys. Plasmas **3**, 2070 (1996).
[9] A.J. Schmitt, A.L. Velikovich, J.H. Gardner, S.P. Obenschain, Y. Aglitskiy, and Y. Chan, Phys. Plasmas **8**, 2287 (2001).
[10] R.H. Lehmberg and S.P. Obenschain, Opt. Commun. **46**, 27 (1983).
[11] S. Skupsky, R.W. Short, T. Kessler, *et al.*, Journ. Appl. Phys. **66**, 3456 (1989).
[12] See EPAPS Document No.E-PHPAEN-8-992105 for "Analysis of intensity structure of the ISI model in the FAST2D hydrocode" by A.J. Schmitt. This document may be retrieved via the EPAPS homepage (http://www.aip.org/pubservs/epaps.html) or from ftp.aip.org in the directory /epaps/.
[13] C.P. Verdon, BAPS **38** 2010 (1993); S.E. Bodner, D.G. Colombant, J.H. Gardner, *et al.*, Phys. Plasmas **5**, 1901 (1998).
[14] A.I. Nikitenko, S.M. Tolokonnikov, and R. Cook, Fusion Tech. **31**, 385 (1997); R.C. Cook, R.L. McEachern, and R.B. Stephens, Fusion Tech. **35**, 224 (1999).
[15] It makes little difference if the initial conditions (surface perturbations) are replaced by local density perturbations that are parallel to the orthogonal mesh but give the same areal mass nonuniformity. In either case, the evolution of the mass quickly results in a sharp density gradient (the ablation surface) that is not aligned on the mesh, and thus sources for nonlinearity.
[16] R. Betti, V.N. Goncharov, R.L. McCrory, and C.P. Verdon, Phys. Plasmas **5**, 1446 (1998).
[17] S.E. Bodner, Phys. Rev. Lett. **33**, 761 (1974); H. Takabe, K. Mima, L. Montierth, and R. L. Morse, Phys. Fluids **28**, 3676 (1985).
[18] S.V. Weber, S.G. Glendinning, D.H. Kalantar, M.H. Key, B.A. Remington, J.E. Rothenberg, E. Wolfrum, C.P. Verdon, and J.P. Knauer, Phys. Plasmas **4**, 1978 (1997).
[19] S.W. Haan, Phys. Rev. A **39**, 5812 (1989).
[20] S.V. Weber, H. Dalhed, D. Eimerl, *et al.*, "Direct Drive Capsules for NIF", University of California report UCRL-LR-105821-97-2 (1997).
[21] A.L. Velikovich, A.J. Schmitt, N. Metzler, and J.H. Gardner, Phys. Plasmas **10**, 3270 (2003).
[22] V.N. Goncharov, J.P. Knauer, P.W. McKenty *et al.*, Phys. Plasmas **10**, 1906 (2003).
[23] K. Anderson and R. Betti, Phys. Plasmas **10**, 4448 (2003).
[24] S.T. Zalesak, *The Applicability of Modern Front-Capturing Methods to the Modeling of Small-Amplitude Instability Growth*, submitted for publication in J. Comput. Phys.
[25] S.K. Godunov, Matematicheskii Sbornik **47**, 271 (1959).